A Phospholipid Bilayer Supported under a Polymerized Langmuir Film

Julie Saccani,* S. Castano,* B. Desbat,* and D. Blaudez[†]

*Laboratoire de Physico-Chimie Moléculaire, Unité Mixte de Recherche 5803 du CNRS; and [†]Centre de Physique Moléculaire Optique et Hertzienne, UMR 5798 du Centre National de la Recherche Scientifique, Université Bordeaux 1, France

ABSTRACT   Phospholipid single bilayers supported on a hydrophilic solid substrate are extensively used in the study of the interaction between model membranes and proteins or polypeptides. In this article, the formation of a single dimyristoylphosphatidylcholine (DMPC) bilayer under an octadecyltrimethoxysilane (OTMS) polymerized Langmuir monolayer at the air-water interface is followed by Brewster angle microscopy (BAM) and polarization-modulated infrared reflection absorption spectroscopy (PM-IRRAS). The formation of the bilayer is initiated by injection of dimyristoylphosphatidylcholine small unilamellar vesicles into the aqueous subphase. Brewster angle microscopy allows visualization of the kinetics of formation and the homogeneity of the bilayer. Spectral simulations of the polarization-modulated infrared reflection absorption spectroscopy spectra reveal that the bilayer thickness is 39 ± 5 Å. This system constitutes the first example of a phospholipid bilayer on a "nanoscopic" support and opens the way to studies involving supported bilayers using powerful experimental techniques such as x-ray reflectivity, vibrational spectroscopies, or Brewster angle microscopy.

INTRODUCTION

Since their introduction in the middle of the 1980s (Brian and McConnell, 1984; Tamm and McConnell, 1985), supported phospholipid bilayers (SPB) have been extensively used in the study of the structure and function of biomembranes (Sackmann, 1996; Boxer, 2000). This system offers numerous advantages relative to other usual model membranes (black lipid membranes and Langmuir films): i), it is composed of two lipid monolayers in a membrane configuration (polar heads toward the outside), ii), membrane proteins can be rather easily incorporated in this architecture, and iii), the presence of an aqueous phase on both sides of the membrane by virtue of the thin water layer ($\sim$2 or 3 nm) that remains between the solid support and the bilayer (Bayerl and Bloom, 1990; Johnson et al., 1991; Charitat et al., 1999; Hughes et al., 2002) increases its biological relevance.

Up to now, classical methods to prepare SPB include i), sequential Langmuir-Blodgett (LB)-Langmuir-Schaeffer (LS) transfer of two monolayers from the air-water interface to a hydrophilic support (Tamm and McConnell, 1985), and ii), adsorption, fusion, and rupture of small unilamellar vesicles (SUV) on a clean hydrophilic support (Brian and McConnell, 1984; Reviakine and Brisson, 2000; Keller et al., 2000). This later method, which results in a fluid (Tamm, 1988; Cézanne et al., 1999; Junglas et al., 2003) and rather homogeneous bilayer (Mou et al., 1994; Egawa and Furusawa, 1999; Jass et al., 2000), is ideal for the incorporation of membrane proteins in the bilayer (Watts et al., 1984; Nakanishi et al., 1985; Contino et al., 1994; Granéli et al., 2003). Some alternatives to these methods were developed later. One can mention i), the "LB/vesicle method," ideal for the fabrication of asymmetric bilayers,

which consists of transfer of a LB monolayer on a solid substrate followed by completion of the bilayer through adsorption of phospholipid molecules from a vesicle solution (Wenzl et al., 1994), and ii), the "floating bilayers," composed of two bilayers obtained by a three-monolayer LB transfer followed by a one-monolayer Langmuir-Schaeffer transfer (Charitat et al., 1999). In all these methods, the most commonly used solid supports are glass, silica, mica, and silicon, the rigidity of which can introduce severe constrains to the bilayer.

Although these SPBs can be physically well characterized by numerous experimental techniques such as atomic force microscopy (AFM), fluorescence microscopy, quartz crystal microbalance, and neutron reflectometry, the hydrophilic support and/or the aqueous subphase are severe drawbacks for studies by infrared (IR) and Raman vibrational spectroscopies (except in the attenuated total reflection configuration, which used a crystal of high refractive index as SPB support) and Brewster angle microscopy (BAM), which are sensitive and nondestructive techniques to get in situ molecular structural, orientational, and morphological information on the bilayer.

To overcome these drawbacks we developed a new fabrication method of SPB compatible for analysis by IR, Raman, and BAM, in which we replace the solid rigid support by a more fluid film polymerized in situ at the air/water interface. Indeed, we demonstrated recently that, under specific conditions, a Langmuir monolayer of octadecyltrimethoxysilane (OTMS) hydrolyses and polymerizes at the water surface (Blaudez et al., 2002). The headgroups of OTMS form a network of Si–O–Si bonds: each polar head forms, on average, two Si–O–Si bonds while one Si–OH bond remains free. Such a monolayer presents a great similarity with a glass surface and thus could be used as a nanoscopic support for SPB.

In this article, we present a polarization-modulated infrared reflection absorption spectroscopy (PM-IRRAS)

---

and a Brewster angle microscopy study of a polymerized OTMS Langmuir monolayer in the presence of dimyristoyl-phosphatidylcholine (DMPC) SUV in the subphase. It is shown that vesicles adsorb at the interface and form a bilayer-thick phospholipidic film. This result is assessed by both spectral simulation of the PM-IRRAS data and by the light intensity of the BAM images.

MATERIALS AND METHODS

Materials

1,2-Dimyristoyl-sn-glycero-3-phosphocholine was purchased from Sigma (Saint Louis, MO), melittin was from SERVA (SERVA Electrophoresis, Heidelberg, Germany), and octadecyltrimethoxysilane and all other chemicals were from Aldrich (Milwaukee, WI). Subphase H_2O, obtained in lab from a MilliQ (Millipore, Molsheim, France) system, presented a nominal resistivity of 18.2 MΩ.cm.

Preparation of a polymerized OTMS monolayer

The preparation and characterization of a polymerized OTMS Langmuir monolayer has been reported recently (Blaudez et al., 2002). Briefly, a Teflon trough with dimensions $9.5 \times 4 \times 1$ cm was filled with a HCl aqueous solution at pH 2. For the experiment with melittin, the solution contained 100 mM NaCl. A total of 15 μl of dilute (10^{-3} M) chloroform solution of OTMS was spread on the subphase to reach a surface pressure of 20 mN/m. The surface pressure was measured with a plate of filter paper held by a Wilhelmy balance (NIMA, Coventry, UK). After waiting 3 h for hydrolysis and polymerization to occur (regularly checked by infrared spectroscopy), 300 μl of a 0.7 M NaOH aqueous solution was injected into the subphase to increase the pH to $\approx$7. During the 3 h wait, the room temperature was gradually increased to 30°C. This temperature was maintained along the course of the experiment.

Small unilamellar vesicles

A dispersion of small unilamellar vesicles was obtained by sonicating 8 mg/ml DMPC in a 20 mM $CaCl_2$ water solution for $\sim$20 min using a Vibracell 75022 sonicator (Bioblock, Illkirch, France) operating in pulsed mode. The solution was then heated to 30°C, above the gel to fluid phase transition temperature ($T_m = 24°C$). A total of 700 μl vesicle solution was injected in the subphase using a Hamilton (Reno, NV) syringe, through the OTMS monolayer and far below the interface. This volume ensures that the total area developed by the vesicles is much larger than the interfacial area delimited by the trough dimensions.

Brewster angle microscopy and infrared spectroscopy

Brewster angle images with dimensions 500×700 μm were recorded using a BAM2+ (NFT, Göttingen, Germany) Brewster angle microscope equipped with a Nd YAG laser doubled in frequency ($\lambda = 532$ nm). The exposure time (ET) was varied from 2×10^{-2} to 2×10^{-3} s depending on the reflected intensity level. The obtained images have been analyzed and processed using the integrated software.

The PM-IRRAS spectra were recorded on a Nicolet (Madison, WI) 870 FT-IR spectrometer with a spectral resolution of 8 cm^{-1}. The details of the optical setup, the experimental procedure, and the two-channel processing of the detected intensity have been already described (Blaudez et al., 1993). To ensure good signal/noise ratio, 600 interferograms representing an

acquisition time of 10 min were coadded. All spectra presented hereafter have been normalized to the spectrum of the bare aqueous subphase.

RESULTS

Brewster angle microscopy

Brewster angle microscopy images obtained at the air-water interface for a polymerized OTMS monolayer in the absence of DMPC vesicles in the subphase, and 4 and 55 min after SUV injection in the subphase, are shown in Fig. 1.

Before SUV injection, the image recorded with an exposure time equal to 2×10^{-2} s shows a monolayer with a curdled structure.

After SUV injection in the subphase, the structure does not evolve but the light intensity of the image significantly increases and the ET has to be gradually decreased to avoid saturation.

In Fig. 2, the light intensity of the image $I(t)$ is plotted as a function of time, the origin corresponding to the injection of the SUV in the subphase. $I(t)$ rapidly increases and reaches a plateau $\sim$30 min after the injection. At longer times, it does not evolve anymore. The behavior of $I(t)$ is correctly reproduced with the following equation:

$$I(t) = I_{initial} + (I_{final} - I_{initial})\left(1 - \exp\left(-\frac{t}{\tau}\right)\right),$$

where $I_{initial}$ is the intensity before injection, and I_{final} is the intensity 55 min after injection. The free parameter is the time constant τ. It is adjusted to 3 min.

The surface pressure (π) at the interface has been recorded during and for long time after Brewster measurements on the same sample (results not shown). It increases almost linearly with time, not only during the first hour after the SUV injection, but also more than 2 h after saturation of the interface, as indicated by the Brewster measurements.

PM-IRRAS measurements

The PM-IRRAS spectrum of a polymerized OTMS monolayer in the absence of DMPC vesicles in the subphase and 30 and 210 min after vesicles injection in the subphase is shown in Fig. 3, A and B. In the 3000–2800 cm^{-1} spectral range (Fig. 3 A), the CH_2 antisymmetric (ν_aCH_2) and symmetric (ν_sCH_2) stretching bands of the methylene groups located at 2918 and 2850 cm^{-1}, respectively, are predominant. Before SUV injection, the two bands clearly arise from the OTMS alkyl chains and have intensities of 8.1×10^{-3} and 5.5×10^{-3}, respectively. After SUV injection, the intensities of both bands rapidly increase during the first minutes (this information is obtained in noisy single-shot spectra not shown here). Thirty minutes after the injection the bands of the CH_2 stretching modes have reached intensities of 1.4×10^{-2} and 9×10^{-3} that hardly increase along the course of the experiment (see Fig. 3 A).
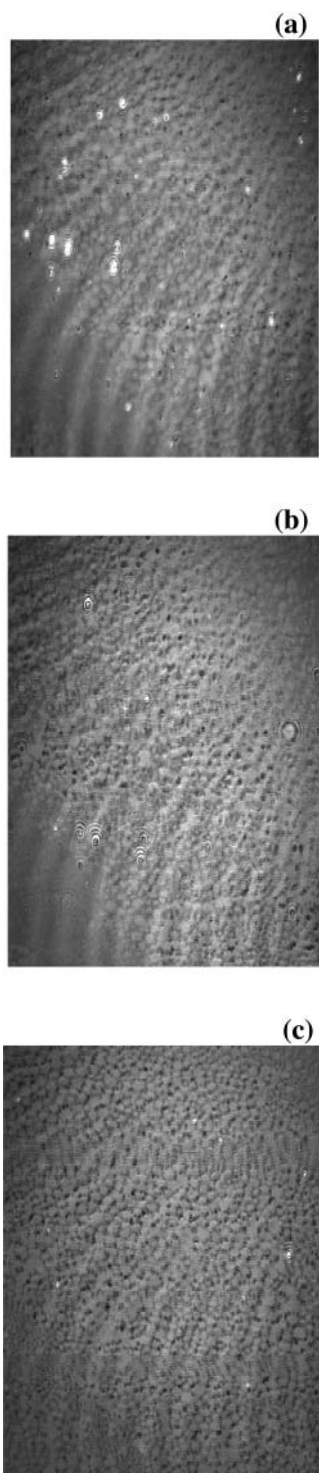
FIGURE 1 Brewster angle microscopy image of an OTMS monolayer (*a*) before SUV injection ($ET = 2 \times 10^{-2}$ s) and (*b*) 4 min ($ET = 4 \times 10^{-3}$ s) and (*c*) 55 min ($ET = 2 \times 10^{-3}$ s) after injection of DMPC SUV in the subphase.
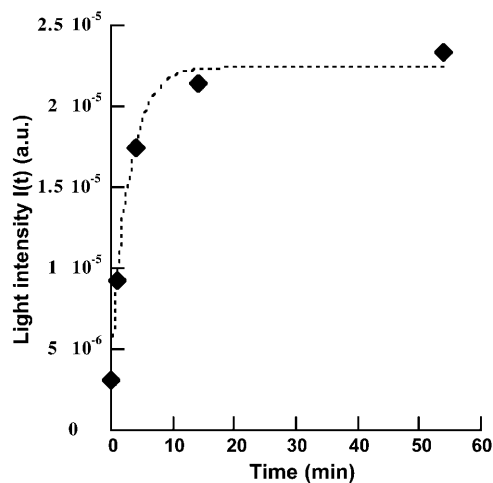

FIGURE 2 Light intensity of the Brewster image as a function of time.

Si–O–Si of siloxane bonds (Socrates, 1980) and a sharp band at 1468 cm^{-1} assigned to the scissoring mode (δCH$_2$) of the OTMS methylene. The broad dip centered at 1660 cm^{-1} is an optical effect peculiar to IRRAS, and it originates from the difference in the optical response for covered and uncovered water surfaces (Blaudez et al., 1996). This effect is particularly pronounced in spectral regions where the aqueous subphase presents an absorption band and therefore a large dispersion of its refractive index. The scissoring mode (δOH$_2$) of liquid water is the cause for the dip at 1660 cm^{-1}.

After SUV injection, new and intense bands located at 1735, 1230, 1089, and 970 cm^{-1} are observed in the PM-IRRAS spectrum (Fig. 3 *B*). These bands are assigned to the C=O stretching (νC = O), the PO$_2$ antisymmetric (ν_aPO$_2$) and symmetric (ν_sPO$_2$) stretching, and the C–N antisymmetric (ν_aCN) stretching in the choline groups, respectively. All these bands thus originate from the DMPC polar headgroups. In addition, the significant increase of the (negative) intensity of the dip at 1660 cm^{-1} shows that the optical thickness of the interfacial molecular film has increased.

Spectral simulations

To determine quantitatively the amount of DMPC that adsorbs at the interface, we have carried out simulations of the PM-IRRAS spectra using software developed in our laboratory (Buffeteau et al., 1999).

In the first step, we calculated the PM-IRRAS spectrum of an OTMS monolayer in the spectral range of the CH$_2$ stretching modes. A Lorentzian shape has been attributed to both bands. The frequency position and width at half intensity were set to the values measured on the corresponding bands in the experimental spectrum recorded before SUV injection in the subphase. The OTMS monolayer was assumed to be uniaxial with the optical axis perpendicular to the interface. The anisotropic optical constants of cadmium
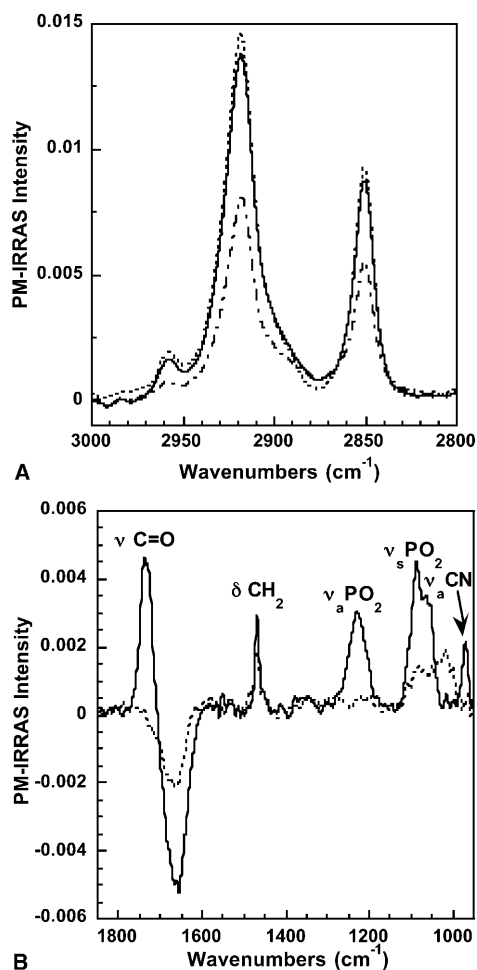
The 1900–900 cm^{-1} spectral range (Fig. 3 *B*) is mainly characteristic of the polar headgroups' vibrational modes. Before SUV injection, one can observe a broad band extending from 950 to 1150 cm^{-1} corresponding to the
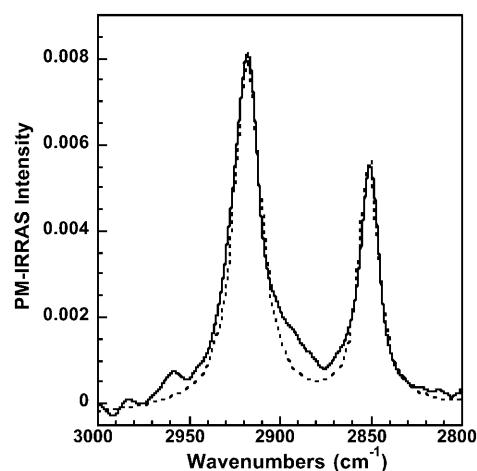
FIGURE 4 Experimental (*solid line*) and calculated (*dotted line*) PM-IRRAS spectrum of a polymerized OTMS monolayer in the absence of DMPC vesicles in the subphase. Calculation has been performed with an OTMS monolayer thickness of 22 Å.

FIGURE 3 (*A*) PM-IRRAS spectrum of a polymerized OTMS monolayer in the absence of DMPC vesicles in the subphase (*dashed-dotted line*), 30 min after injection of DMPC vesicles into the subphase (*solid line*), and 210 min after injection of DMPC vesicles into the subphase (*dotted line*). (*B*) PM-IRRAS spectrum of a polymerized OTMS monolayer in the absence of DMPC vesicles in the subphase (*dotted line*) and 30 min after injection of DMPC vesicles into the subphase (*solid line*).

For DMPC we used anisotropic optical constants determined experimentally (unpublished results). Their values were carefully checked using experimental and calculated spectra of DMPC monolayers at the air-water interface. The result of the calculation using a 39-Å DMPC thickness reported in Fig. 5 shows a very good agreement with the experiment. The calculation using DMPC thickness of 34 and 44 Å is presented in the $\nu_a CH_2$ spectral domain (Fig. 5, *inset*). With regard to these results, the DMPC layer thickness is estimated to 39 ± 5 Å.

arachidate (Buffeteau et al., 1999) whose alkyl chain has the same length as OTMS have been used in the calculation. Finally the thickness of the monolayer had to be adjusted to 22 Å to fit the experimental intensities (Fig. 4). This thickness may appear low compared to the 26 Å determined previously by Parikh et al. (1997). However, PM-IRRAS intensity is very sensitive to molecular orientation through a specific surface selection rule (Blaudez et al., 1996). The apparent discrepancy noticed here can be explained by a tilt of the alkyl chains by ~20° from the normal to the interface. Such a molecular reorientation of OTMS molecules at the water surface induced by the polymerization has already been qualitatively described (Blaudez et al., 2002).

In the second step, we simulated the PM-IRRAS spectrum of the OTMS monolayer at 90 min after injection of DMPC vesicles into the subphase. In this calculation, we added a DMPC layer under the above-described OTMS monolayer.
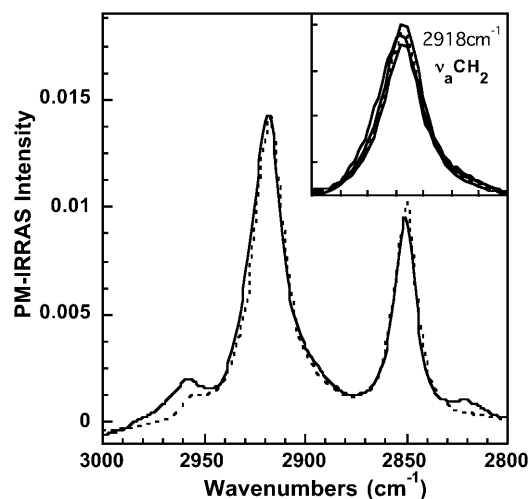

FIGURE 5 Experimental (*solid line*) and calculated (*dotted line*) PM-IRRAS spectrum of a polymerized OTMS monolayer 90 min after injection of DMPC vesicles into the subphase. Calculation has been performed with an OTMS monolayer thickness of 22 Å and a DMPC thickness of 39 Å. (*Inset*) Calculation with a DMPC thickness of 34 and 44 Å are shown together with the experimental and calculated spectra of the main figure, in the antisymmetric $\nu_a CH_2$ stretching band domain.

DISCUSSION

Using Brewster angle microscopy and Polarization Modulation IRRAS, we have investigated the changes that occur at the air-water interface in the presence of a polymerized OTMS monolayer when DMPC small unilamellar vesicles are injected into the aqueous subphase.

The Brewster images indicate that, within the optical resolution ($\sim 1\ \mu$m), a homogeneous layer of DMPC forms in the vicinity of the interface, as shown by the global increasing of the intensity without modification of the initial curdled structure. This does not exclude the possible presence of smaller defects (holes for example) in the layer. On the other hand, due to the high sensitivity of BAM to film thickness, it is possible to rule out the presence of domains with large thickness or aggregates that would lead to very bright spots. From this, we can estimate the DMPC layer thickness using the light intensity before ($I_{initial}$) and 55 min after SUV injection (I_{final}). The experimental ratio $I_{final}/I_{initial}$ is equal to 6.92. This means that the interfacial film thickness has been multiplied by a factor of 2.63 between the initial and final states, as the light intensity of a Brewster image is proportional to the square of the film thickness (de Mul and Mann, 1998). In this calculation, we assume that the optical index of the film at the interface varies little after the SUV injection. This assumption is possible because OTMS and DMPC have both an optical index close to 1.5 at $\lambda = 532$ nm and also because the presence of a thin water layer between OTMS and DMPC modifies very little the p-polarized reflectivity R_p at the Brewster angle of water. Calculation demonstrates that the variation of R_p does not exceed 1% when the water layer is up to 30-Å thick. This factor of 2.63 allows an estimation of 36 Å of the DMPC layer thickness, taking 22 Å for the OTMS monolayer. This result is in good agreement with spectral simulations of the PM-IRRAS spectra that give a thickness of ~ 39 Å for this DMPC layer. Recently, Hughes et al. (2002) measured the thickness of a supported DMPC bilayer by neutron reflectivity. They found values of 42 Å for the bilayer in the gel phase and 35 Å for the bilayer in the fluid phase. Our measurements were performed at 30°C, far above the temperature of the gel to fluid phase transition ($T_m = 24$°C). However, the frequency position and width at half intensity of the $\nu_a CH_2$ (2919 $\pm$ 0.2 and 22 cm^{-1}, respectively) and $\nu_s CH_2$ (2850.6 $\pm$ 0.2 and 13 cm^{-1}, respectively) bands coming from the DMPC alone (this spectrum, not shown, is obtained by subtracting the spectrum of the OTMS monolayer from the total spectrum) indicate that little conformational defects are present in the phospholipid alkyl chains (Flach et al., 1993) as observed in gel phase. This contradictory feature should be explained by a phase behavior modification induced by specific interaction with the OTMS support. The kinetics of formation of the DMPC layer under the polymerized Langmuir OTMS monolayer have been deduced from Brewster angle microscopy data. The results show that the formation of the DMPC layer occurs mainly within 15 min after the injection of SUV in the subphase (Fig. 2). This time scale corresponds to the time required for the formation of a supported egg-PC bilayer on SiO$_2$ by fusion and rupture of SUV, as measured by quartz crystal microbalance and surface plasmon resonance (Keller et al., 2000). However, a single exponential function does not perfectly fit the experimental behavior of $I(t)$ at longer times (Fig. 2). In particular, $I(t)$ continues to slowly increase after the saturation expected from the fit. This observation may be interpreted as a filling of hole defects in the DMPC bilayer. Such holes and their further completion have been observed in mica-supported bilayers by atomic force microscopy (Reviakine and Brisson, 2000). Even if surface pressure measurements are difficult to interpret in such a multilayered system at the air-water interface, the regular increase of π after vesicle injection is certainly significant of adsorption of DMPC molecules under the OTMS monolayer. The increase of π long after SUV injection is therefore consistent with a progressive completion of hole defects in the lipid bilayer.

In summary, our experimental observations are consistent with the formation of a DMPC bilayer supported under the OTMS monolayer polymerized at the air-water interface. This bilayer would form largely according to the same process of SUV rupture as it occurs with macroscopic hydrophilic solid supports. In addition, it is likely that the 2–3-nm thick water layer that separates a SPB from its solid support (Bayerl and Bloom, 1990; Johnson et al., 1991) also exists in this case of a polymerized Langmuir monolayer support. However, the detection of this water layer is not accessible with the experimental methods used in this article. It would require the use of a technique that is sensitive to hydrogen atoms such as neutron reflectivity.

It is thus likely that this bilayer supported under a Langmuir film represents a membrane model with properties (hydration, fluidity, structure) close to that of natural membranes. It could be used to investigate the mechanisms of interaction between peptides or proteins and membranes. As very preliminary illustration, we studied by PM-IRRAS the interaction between a DMPC supported bilayer and melittin, a widely studied lytic amphipathic peptide from bee venom. The spectra of the bilayer before and after injection of melittin into the subphase are presented in Fig. 6. The quantity of injected peptide corresponds to a 1:72 peptide/lipid molar ratio, taking into account the excess of lipid vesicles remaining in the subphase. Even with this relatively low peptide/lipid ratio we can notice a significant modification of the intensity of the lipid headgroup absorption bands. After peptide injection, the C=O stretching band decreases while the PO$_2$ stretching bands increase. This indicates a reorientation of the DMPC headgroups in the presence of melittin. On the other hand, the CH$_2$ stretching bands are hardly modified (*inset* in Fig. 6), indicating that melittin very slightly perturbs the aliphatic chains. From this very
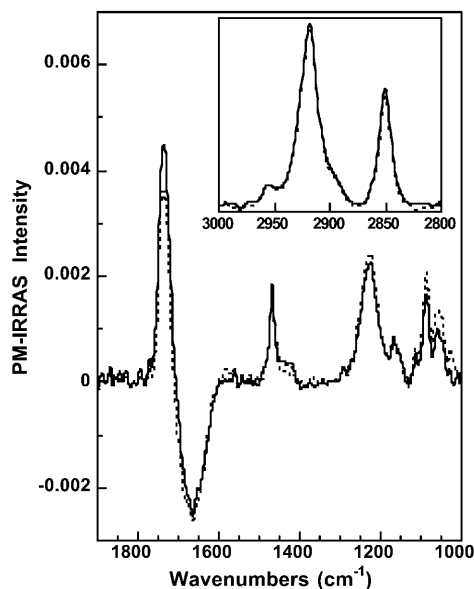
FIGURE 6   PM-IRRAS spectrum in the 1850–950 cm^{-1} and 3000–2800 cm^{-1} spectral ranges of a DMPC bilayer supported under a polymerized OTMS monolayer before (*solid line*) and after (*dotted line*) injection of melittin into the subphase.

preliminary result, further work with improved experimental conditions is planned. In particular, a specific trough will be constructed to purge the subphase of excess vesicles before peptide injection.

CONCLUSIONS

In this article we show that a DMPC bilayer can be formed under a polymerized OTMS Langmuir monolayer at the air-water interface by injection of small unilamellar vesicles of the phospholipid into the aqueous subphase. Brewster angle microscopy has allowed visualization of the kinetics of formation and the homogeneity of the bilayer while polarization modulated infrared spectroscopy together with spectral simulations have given a value of 39 ± 5 Å for its thickness.

Phospholipid single bilayers on a solid support are extensively used in the study of the interactions between model membranes and proteins or polypeptides. The possibility of fabricating single bilayers in an aqueous environment and on a nanoscopic support opens the way to their characterization by powerful experimental techniques such as x-ray reflectivity, vibrational spectroscopies, or Brewster angle microscopy that have not yet been available. Furthermore, this supported single bilayer offers a high potentiality to investigate model membranes that closely mimic natural systems. Indeed, it would be possible to modulate the composition of the vesicle membrane by introduction of charged lipids or cholesterol, for instance, and to build proteoliposomes to fuse directly at the OTMS interface. Therefore, this new system appears to be a promising tool for the in situ study and the understanding of protein/membrane interactions.

REFERENCES

Bayerl, T. M., and M. Bloom. 1990. Physical properties of single phospholipid bilayers adsorbed to micro glass beads. *Biophys. J.* 58:357–362.

Blaudez, D., M. Bonnier, B. Desbat, and F. Rondelez. 2002. Two dimensional polymerization in Langmuir films: a PM-IRRAS study of octadecyltrimethoxysilane monolayers. *Langmuir.* 18:9158–9163.

Blaudez, D., T. Buffeteau, J.-C. Cornut, B. Desbat, N. Escafre, M. Pézolet, and J.-M. Turlet. 1993. Polarization-Modulated FT-IR spectroscopy of a spread monolayer at the air/water interface. *Appl. Spectrosc.* 47: 869–874.

Blaudez, D., J.-M. Turlet, J. Dufourcq, D. Bard, T. Buffeteau, and B. Desbat. 1996. Investigations at the air/water interface using polarization modulation IR spectroscopy. *J. Chem. Soc. Faraday Trans.* 92:525–530.

Boxer, S. G. 2000. Molecular transport and organization in supported lipid membranes. *Curr. Opin. Chem. Biol.* 4:704–709.

Brian, A. A., and H. M. McConnell. 1984. Allogeneic stimulation of cytotoxic T cells by supported planar membranes. *Proc. Natl. Acad. Sci. USA.* 81:6159–6163.

Buffeteau, T., D. Blaudez, E. Péré, and B. Desbat. 1999. Optical constant determination in the infrared of uniaxially oriented monolayers from transmittance and reflectance measurements. *J. Phys. Chem. B.* 103:5020–5027.

Cézanne, L., A. Lopez, F. Loste, G. Parnaud, O. Saurel, P. Demange, and J.-F. Tocanne. 1999. Organization and dynamics of the proteolipid complexes formed by annexin V and lipids in planar supported lipid bilayers. *Biochemistry.* 38:2779–2786.

Charitat, T., E. Bellet-Amalric, G. Fragneto, and F. Graner. 1999. Adsorbed and free lipid bilayers at the solid-liquid interface. *Eur. Phys. J. B.* 8:583–593.

Contino, P. B., C. A. Hasselbacher, J. B. A. Ross, and Y. Nemerson. 1994. Use of an oriented transmembrane protein to probe the assembly of a supported phospholipid bilayer. *Biophys. J.* 67:1113–1116.

De Mul, M. N. G., and J. A. Mann, Jr. 1998. Determination of the thickness and optical properties of a Langmuir film from domain morphology by Brewster angle microscopy. *Langmuir.* 14:2455–2466.

Egawa, H., and K. Furusawa. 1999. Liposome adhesion on mica surface studied by atomic force microscopy. *Langmuir.* 15:1660–1666.

Flach, C. R., J. W. Brauner, and R. Mendelsohn. 1993. Calcium ion interactions with insoluble phospholipid monolayer films at the A/W interface. External reflection-absorption IR studies. *Biophys. J.* 65:1994–2001.

Granéli, A., J. Rydström, B. Kasemo, and F. Höök. 2003. Formation of supported lipid bilayer membranes on SiO2 from proteoliposomes containing transmembrane proteins. *Langmuir.* 19:842–850.

Hughes, A. V., S. J. Roser, M. Gerstenberg, A. Goldar, B. Stidder, R. Feidenhans, and J. Bradshaw. 2002. Phase behavior of DMPC free bilayers studied by neutron reflectivity. *Langmuir.* 18:8161–8171.

Jass, J., T. Tjärnhage, and G. Puu. 2000. From liposomes to supported, planar bilayer structures on hydrophilic and hydrophobic surfaces: an atomic force microscopy study. *Biophys. J.* 79:3153–3163.

Johnson, S. J., T. M. Bayerl, D. C. McDermott, G. W. Adam, A. R. Rennie, R. K. Thomas, and E. Sackmann. 1991. Structure of an adsorbed dimyristoylphosphatidylcholine bilayer measured with specular reflection of neutrons. *Biophys. J.* 59:289–294.

Junglas, M., B. Danner, and T. M. Bayerl. 2003. Molecular order parameter profiles and diffusion coefficients of cationic lipid bilayers on a solid support. *Langmuir.* 19:1914–1917.

Keller, C. A., K. Glasmästar, V. P. Zhdanov, and B. Kasemo. 2000. Formation of supported membranes from vesicles. *Phys. Rev. Lett.* 84:5443–5446.

Mou, J., J. Yang, and Z. Shao. 1994. Tris(hydroxymethyl)aminomethane ($C_4H_{11}NO_3$) induced a ripple phase in supported unilamellar phospholipid bilayers. *Biochemistry.* 33:4439–4443.

Nakanishi, M., K. Matsumoto, and S. Takahashi. 1985. Binding of macrophages and phospholipid flip-flop in supported lipid bilayers. *FEBS Lett.* 192:66–70.

Parikh, A. N., M. A. Schivley, E. Koo, K. Seshadri, D. Aurentz, K. Mueller, and D. L. Allara. 1997. *n*-Alkylsiloxanes: from single monolayers to layered crystals. The formation of crystalline polymers from the hydrolysis of *n*-Octadecyltrichlorosilane. *J. Am. Chem. Soc.* 119: 3135–3143.

Reviakine, I., and A. Brisson. 2000. Formation of supported phospholipid bilayers from unilamellar vesicles investigated by atomic force microscopy. *Langmuir.* 16:1806–1815.

Sackmann, E. 1996. Supported membranes: scientific and practical applications. *Science.* 271:43–48.

Socrates, G. 1980. Infrared Characteristic Group Frequencies. John Wiley and Sons, New York.

Tamm, L. K. 1988. Lateral diffusion and fluorescence microscope studies on a monoclonal antibody specifically bound to supported phospholipid bilayers. *Biochemistry.* 27:1450–1457.

Tamm, L. K., and H. M. McConnell. 1985. Supported phospholipid bilayers. *Biophys. J.* 47:105–113.

Watts, T. H., A. A. Brian, J. W. Kappler, P. Marrack, and H. McConnell. 1984. Antigen presentation by supported planar membranes containing affinity-purified I-A[d]. *Proc. Natl. Acad. Sci. USA.* 81:7564–7568.

Wenzl, P., M. Fringeli, J. Goette, and U. P. Fringeli. 1994. Supported phospholipid bilayers prepared by the ''LB/vesicle method'': a Fourier transform infrared attenuated total reflection spectroscopic study on structure and stability. *Langmuir.* 10:4253–4264.